Acta Cardiol Sin 2019;35:65–74
Original Article
doi: 10.6515/ACS.201901_35(1).20180731A

Basic Science

Inhibitory Effect of Photodynamic Therapy with Indocyanine Green on Rat Smooth Muscle Cells

Jih-Shyong Lin,[1,2] Chia-Jung Wang[2] and Wen-Tyng Li[2,3]

Background: Vascular smooth muscle cells play a critical role in the intimal hyperplasia of restenosis. A previous study of a rat balloon injury model demonstrated that photodynamic therapy (PDT) using indocyanine green (ICG) and near-infrared (NIR) light irradiation reduced intimal hyperplasia in carotid arteries. However, the effect of ICG-PDT on smooth muscle cells remains unclear. This study aimed to evaluate the effects of PDT with ICG and NIR irradiation on the viability of vascular smooth muscle (A-10) cells.

Methods: A-10 cells were incubated with ICG at different concentrations for different time intervals. Intracellular accumulation of ICG inside the cells was observed by light microscopy, ultraviolet-visible (UV-VIS) spectrophotometry and spectrofluorometry. Cell viability and cell death after ICG-PDT were assessed by 3-(4,5-dimethylthiazol-2-yl)-2,5-diphenyltetrazolium bromide assay and lactate dehydrogenase release assay. Changes in nuclear morphology and cell cycle distribution were evaluated to determine the possible cell death mechanism mediated by ICG-PDT.

Results: ICG uptake in A-10 cells increased with the amount of ICG in the culture media. The intracellular accumulation of ICG reached a maximum at 8 h. After ICG-PDT, cell viability decreased and cell death increased in a concentration-dependent manner. The half maximal inhibitory concentration of ICG was 8.3 μM with 4 J/cm^2 NIR irradiation. Membrane blebbing and chromatin condensation were observed, and the percentage of cells in the sub-G_1 phase increased after ICG-PDT. Thus, apoptosis might be responsible for decreasing the viability of A-10 cells by ICG-PDT.

Conclusions: This study demonstrated that ICG-PDT had an inhibitory effect on smooth muscle cells, possibly via an apoptosis pathway.

Key Words: Cell viability • Indocyanine green • Near-infrared • Photodynamic therapy • Smooth muscle cell

INTRODUCTION

Vascular smooth muscle cells are the major cell type within blood vessels. Smooth muscle cells in the arterial tunica media of normal vessels behave differently from those in the intima of developing atheroma,[1,2] and they exhibit low rates of proliferation, migration and apoptosis in normal blood vessels. In the process of atherosclerosis, changes in the composition and structure of blood vessel walls are entirely due to increased proliferation, migration and apoptosis rates of smooth muscle cells.[3] Accumulation of smooth muscle cells is a result of a struggle between death and procreation in the progression of atheroma.[4] Extracellular matrix produced by smooth muscles cells in the process of atheroma formation are known to be the most important contributor to the production of connective tissue in vessels.[4] Smooth muscle cells are also associated with the formation of atheroma in the late stage,[5,6] and they can be activated by cholesterol loading to differentiate into a macrophage-like state, and participate in the initiation of atherosclerotic lesions.[6]

Balloon angioplasty and stents are widely used in the clinical treatment of coronary artery diseases. How-

Received: May 3, 2018 Accepted: July 31, 2018
[1]Division of Cardiology, Department of Internal Medicine, Taoyuan General Hospital, Ministry of Health and Welfare; [2]Department of Biomedical Engineering; [3]Center for Biomedical Technology and Center for Nanotechnology, Chung Yuan Christian University, Taoyuan, Taiwan.
Corresponding author: Dr. Wen-Tyng Li, Department of Biomedical Engineering, Chung Yuan Christian University, Taoyuan 320, Taiwan.
Tel: 886-3-265-4543; Fax: 886-3-265-4599; E-mail: wtli@cycu.edu.tw

ever, the vessel lumen often re-narrows within 6 months after treatment due to mechanical damage induced by stent implantation or balloon angioplasty. The rate of restenosis is around 10% even after the implantation of drug-eluting stents.[7-10] The mechanism of restenosis is similar to that of wound healing.[11,12] After the intima is injured, inflammatory reactions cause the proliferation and migration of smooth muscle cells within the media and the intima, leading to intimal hyperplasia.[13,14] Therefore, therapies that modulate the proliferation, migration and apoptosis of smooth muscle cells may be useful for inhibiting restenosis after treatment for atherosclerosis.

Photodynamic therapy (PDT) is a treatment modality involving the combined use of a photosensitizer, light and oxygen. Photosensitizers are activated by light at a specific wavelength and react with nearby oxygen in the tissue to generate reactive oxygen species (ROS), thereby resulting in cell death in the lighted area. PDT is widely used in cancer therapy.[15] Although it has not been used as a treatment modality for cardiovascular diseases, several clinical trials have demonstrated that PDT was effective in reducing atherosclerotic lesions and inhibiting plaque progression by stabilizing atherosclerotic plaques.[16-21] PDT has also been shown to prevent intimal hyperplasia in balloon-injured arteries by suppressing smooth muscle cell proliferation, and modulating adventitial fibroblast function to generate a matrix barrier to invasive vascular cell migration.[22-25] It has also been demonstrated that PDT can induce the apoptosis of vascular smooth muscle cells in a light-energy and photosensitizer concentration-dependent manner.[26] However, the efficacy of PDT in the treatment of intimal hyperplasia is hampered by poor penetration depth of visible light into tissue in order to excite most photosensitizers.

Indocyanine green (ICG), a near-infrared (NIR) excitable fluorophore which allows for deeper light penetration into tissue, is used in clinical diagnosis and fluorescence angiography.[27] It has also been used as a photosensitizer to treat murine mammary tumors and metastatic tumors.[28,29] ICG-PDT has been shown to be effective in killing skin-associated microorganisms.[30-32] Our recent study showed that ICG-PDT using a light dose of 4 J/cm^2 was effective in suppressing intimal hyperplasia in a rat model with balloon-injured carotid arteries.[33] Smooth muscle cells play an important role in the initiation of atheroma and the process of restenosis, however it remains unclear whether vascular smooth muscle cells are affected by ICG-PDT. In this study, the effects of PDT with ICG and NIR light emitting diode (LED) irradiation on the viability of vascular smooth muscle (A-10) cells were evaluated.

MATERIALS AND METHODS

Chemicals

ICG, the photosensitizer used in this study, was purchased from Tokyo Chemical Industry, Co. Ltd. (Japan). It was freshly prepared in phosphate-buffered saline (PBS) at a concentration of 1 mg/mL before use. All chemicals were purchased from Sigma-Aldrich Corp. (MO, USA). Cell culture reagents and cell culture vessels were purchased from Thermo Fisher Scientific Inc. (CA, USA). A CytoTox 96® non-radioactive cytotoxicity assay kit was purchased from Promega Corp. (MI, USA).

Cell line

The A-10 (ATCC #: CRL-1476) smooth muscle cell line derived from thoracic aorta of *Rattus norvegicus*, was obtained from the Bioresource Collection and Research Center (BCRC, Hsinchu, Taiwan). Cells were cultured in Dulbecco's Modified Eagle Medium (DMEM) with 4 mM L-glutamine adjusted to contain 1.5 g/L sodium bicarbonate, 4.5 g/L glucose, 1.0 mM sodium pyruvate, 10 IU penicillin, 10 μg/mL streptomycin and 10% fetal bovine serum (FBS). The cells were grown at 37 °C in a humidified atmosphere with 5% CO_2.

Intracellular accumulation of indocyanine green

A-10 cells were seeded at a density of 2,500 cells/cm^2 in a 6-well culture plate. After 24 h, the medium was changed to DMEM containing 2% fetal bovine serum (FBS). The cells were incubated for 24 h with ICG concentrations ranging from 1 to 50 μM in a dark humid atmosphere containing 5% CO_2. The medium was then removed and the cell monolayer was washed with PBS. The presence of ICG inside the cells was assessed using an inverted microscope (Eclipse TS100-F; Nikon Instruments Inc., Japan).

The accumulation of 20 μM ICG was studied as a function of incubation in the 0 to 24 h range to deter-

mine the optimal timing of light application for PDT. The medium was subsequently removed, and the cells were washed twice with PBS. The cells were then detached using a cell scraper and disrupted in PBS using an ultrasonic processor (VCX 130 PB; Sonics & Materials, Inc., CT, USA). Cell lysates were centrifuged at 10,000 × g for 10 min to remove cell debris. The protein content of cell lysates was determined using the bicinchoninic acid (BCA) assay. Intracellular ICG accumulation was evaluated by both absorbance at 780 nm and fluorescence emission at 830 nm. The absorbance of ICG in cell lysates was measured using an ultraviolet-visible (UV-VIS) spectrophotometer (GENESYS™ 10S; Thermo Fisher Scientific Inc., CA, USA). The fluorescence intensity of ICG was quantitated using a spectrofluorometer (FluoroMax®-4; HORIBA, Ltd., Japan). The uptake of ICG by cells was expressed as either absorbance intensity or fluorescence intensity of the photosensitizer per milligram of protein.

Light source and photodynamic treatment

A custom-made NIR light source composed of 4 × 4 LED lamps (ShenZhen UGet Optoelectronics Co., Ltd., Guangdong, China) with a wavelength ranging from 760 nm to 780 nm was used for photodynamic treatment. The irradiance at the surface of the cell monolayer was 5 mW/cm^2 measured using a power meter (Orion, Ophir Optronics Ltd., UT, USA). The radiant exposure (J/cm^2) could be adjusted according to the duration of LED irradiation.

In the PDT procedure, A-10 cells were first put in DMEM with 10% FBS in a 5% CO_2 atmosphere at 37 °C and allowed to adhere for 24 h. After rinsing with PBS, the cells were allowed to incubate with DMEM containing 2% FBS and different concentrations (6~48 μM) of ICG for 8 h. Afterwards, ICG-containing media were removed, and the cells were rinsed with PBS again and refed with fresh DMEM without ICG. The A-10 cells were then illuminated in darkness using our custom-made NIR light source at a total radiant exposure of 2 and 4 J/cm^2 at room temperature and atmosphere. Cells without LED exposure or ICG incubation placed under the same conditions were used as the untreated controls.

Cell viability assay

A-10 cells were seeded at a density of 20,000 cells/cm^2 in 48-well cell culture plates. After PDT, the cells were incubated in 2% FBS-containing media for 24 h and then subjected to cell viability assay. The viability of cells was assessed using the 3-(4,5-dimethylthiazol-2-yl)-2,5-diphenyltetrazolium bromide (MTT) assay, which measures the capacity of mitochondrial dehydrogenase in viable cells to reduce MTT to a purple formazan precipitate. The cells were incubated with MTT solution (0.5 mg/mL) at 37 °C for 4 h. The purple formazan formed in each well was dissolved in 250 μL dimethyl sulfoxide solution for 10 min. The absorbance at 570 nm was measured using a plate reader (Multiskan® Spectrum; Thermo Fisher Scientific Inc., CA, USA). The viability of the A-10 cells was based on the results of three separate runs, in which the experiment was performed in triplicate in each run. The results were given as the percentage of the data obtained with control cultures.

Cytotoxicity assay

A-10 cells were seeded at a density of 3,000 cells/cm^2 in 48-well cell culture plates. After PDT, the cells were incubated in 2% FBS-containing media for 24 h and then subjected to cytotoxicity analysis. Quantitative assessment of cell death was evaluated using a lactate dehydrogenase (LDH) assay with a CytoTox 96® non-radioactive cytotoxicity assay kit. LDH is released from the cytoplasm into the culture medium as a result of cell membrane damage and cell lysis by PDT. LDH can convert a tetrazolium salt into a red formazan product with absorbance at 490 nm. The LDH assay was performed according to the manufacturer's instruction. Maximal release was obtained after treating the control cells with 1% Triton X-100 at 37 °C for 45 min. The absorbance at 490 nm for each sample and maximal release was measured using a plate reader. The LDH release percentage was expressed using the formula: (sample value/maximal release) × 100%. The cytotoxicity after PDT was based on the results of three separate runs, in which the experiment was performed in triplicate in each run.

Nuclear assessment using Hoechst stain

A-10 cells were seeded at a density of 12,500 cells/cm^2 in a 35-mm culture dish and treated with an optimal inhibitory concentration of ICG (9 μM). After 8 h of incubation, the cells were treated with 4 J/cm^2 NIR irradiation. After 45 min, the cells were stained with 0.04

μg/mL Hoechst 33258 stain at room temperature for 30 min. The cells were then rinsed with PBS and examined under an inverted fluorescence microscope (DM1L; Leica Microsystems, GmbH, Germany).

Cell cycle analysis using flow cytometry

A-10 cells were seeded at a density of 20,000 cells/cm^2 in a 10-cm culture dish and treated with 6 μM ICG for 8 h. The cells were subjected to PDT at 2 J/cm^2 and collected at 12 h post PDT. The cells were trypsinized and washed twice with ice cold PBS and fixed at 4 °C in 70% ethanol for 24 h. The fixed cells were resuspended with a staining solution consisting of 50 μg/mL propidium iodide (PI), 0.1% Triton X-100 and 50 μg/mL RNase in PBS. The samples were then incubated at 4 °C for 30 min. Flow cytometry was performed on a FACSCalibur flow cytometer (BD Biosciences, NJ, USA).

Statistical analysis

The results are expressed as mean ± standard error of the mean. Statistical analysis of the data was performed using GraphPad InStat®, version 3.05 (GraphPad Software, CA, USA). The Kruskal-Wallis test was used to compare medians between the control, light, ICG and ICG + light groups. A p-value of less than 0.05 was considered to indicate a significant difference between the medians of all groups.

RESULTS

Intracellular accumulation of indocyanine green

The effect of ICG concentration on the uptake of ICG by smooth muscle (A-10) cells after 24 h of incubation is shown in Figure 1. When incubated with 10 μM ICG, light greenish staining of the cells could be seen under the inverted microscope. The intensity of ICG staining increased with the photosensitizer concentration in the incubation medium. In cultures exposed to 50 μM ICG (Figure 1D), some cells with intense staining had a shrunken morphology.

ICG has an NIR absorbance peak at around 780 nm and fluorescence emission peak at 830 nm. Therefore, the absorbance intensity at 780 nm and fluorescence intensity at 830 nm were used to measure the dose of ICG within the A-10 cells. In order to detect apparent optical signals of ICG from the cell lysates, an ICG concentration of 20 μM was selected for the experiments of uptake kinetics. The time course of intracellular accumulation of ICG is presented in Figure 2. Both the fluorescence intensity and absorbance intensity of ICG increased with the incubation time and reached a plateau at 8 h. Therefore, NIR light for PDT was illuminated after 8 h exposure to ICG for the rest of the experiments.

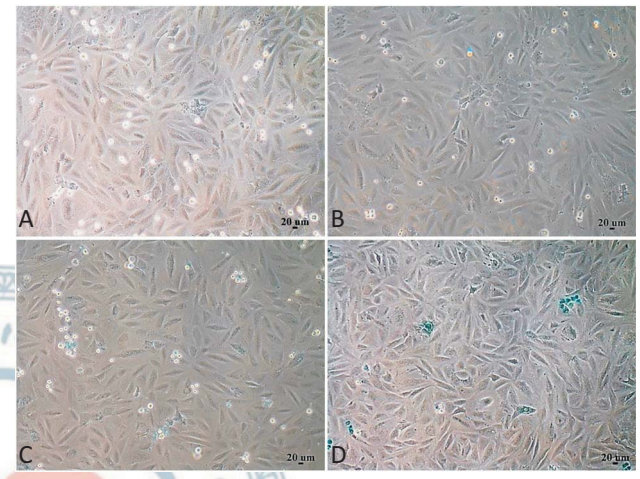

Figure 1. *Phase-contrast micrographs of rat smooth muscle (A-10) cells after 24-h incubation with indocyanine green (ICG). A-10 cells were exposed to ICG for 24 h and observed under a phase-contrast microscope. There were more cells with green-color staining in cultures exposed to higher concentration of ICG. ICG concentration: 0 μM (A), 1 μM (B), 10 μM (C) and 50 μM (D). Original magnification 100x.*

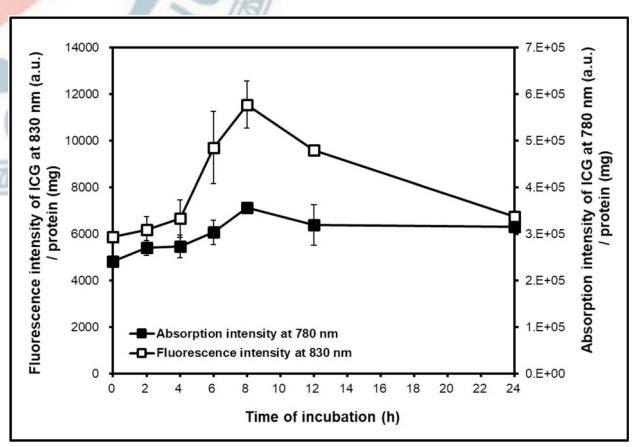

Figure 2. *Intracellular uptake of indocyanine green (ICG) in rat smooth muscle (A-10) cells as a function of incubation time. A-10 cells were exposed to 20 μM ICG for up to 24 h. The ICG uptake was measured by using the optical absorption of ICG at 780 nm (■) and fluorescence emission at 830 nm (□). Intracellular ICG level was expressed as normalized absorption intensity or fluorescence intensity per mg protein measured in cell extract. Values represent mean ± standard error of three separate experiments.*

Effect of photodynamic treatment on cell viability and cell death

To determine the effect of the concentration of ICG on A-10 cells, cell viability was evaluated using the MTT assay, and cell death was determined by measuring LDH activity in the culture medium. The percentage of cell viability was measured by normalizing the results of the MTT assay with control cells (without ICG or light exposure). As shown in Figure 3, cell viability decreased in a concentration-dependent manner after 8 h of incubation with the photosensitizer and then exposure to light. Cell viability was around 48% at 9 μM ICG and 4 J/cm^2 light irradiation. Exposure to 12 μM ICG and light irradiation further reduced cell viability to 21%. The half maximal inhibitory concentration (IC_{50}) of ICG under light irradiation was 8.3 μM.

The effect of ICG concentration on cell death was almost opposite to that on cell viability (Figure 4). Cell death increased in a dose-dependent manner after ICG-PDT, and was around 28% at 6 μM ICG and 4 J/cm^2 light irradiation. The LDH release rate increased to 61% at 9 μM ICG and 73% at 12 μM ICG with light irradiation.

Cell viability and cell death of the ICG-exposed cells without illumination was not different from the control cells. ICG had no darkness toxicity to the A-10 cells. In addition, a lower ICG concentration (12 μM) tended to increase cell viability (140%). Similar observations have been reported in other *in vitro* studies.[34,35] It is possible that ICG treatment alone may result in increased activity of mitochondrial reductase as an early response to stress.

Nuclear assessment after photodynamic treatment

Blue Hoechst 33258 staining was used to assess the change in nuclear morphology 45 min after PDT at 9 μM ICG and 4 J/cm^2 light irradiation, and was compared to the untreated control cells.[36] Phase-contrast images (Figure 5) showed dense spherical nuclei without any damage in the control cells, while the PDT-treated cells showed nuclear shrinkage with the nuclei becoming smaller and membrane blebbing. As shown in the fluorescence images (Figure 5), most of the control cells were not stained well with Hoechst 33258, and only a few apoptotic control cells were stained with blue fluorescence dye. However, in the ICG-PDT group, many cells exhibited blue fluorescence, which suggested the involvement of DNA damage.

Cell cycle change after photodynamic treatment

To understand the mechanism by which PDT inhibited A-10 cell viability, the effect of PDT (6 μM ICG and 2 J/cm^2 light irradiation) on cell cycle distribution was analyzed by flow cytometry. As shown in Figure 6, no substantial differences in the medians of the control, light, ICG and ICG + light (PDT) groups were observed when comparing the cell proportions at the G_0/G_1, S and G_2/M

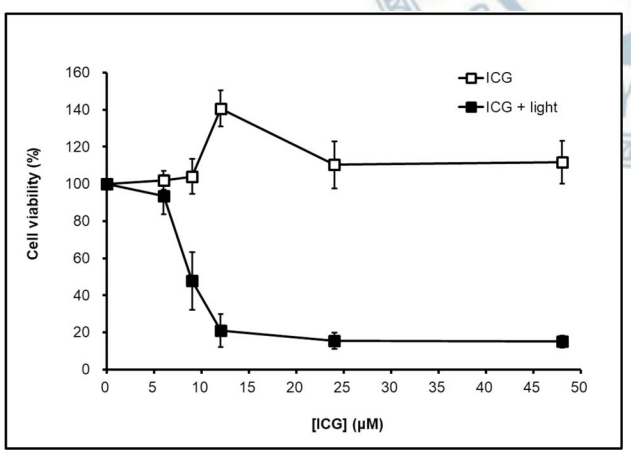

Figure 3. *Cell viability of rat smooth muscle (A-10) cells after photoactivation of indocyanine green (ICG). A-10 cells were incubated for 8 h in the presence of different concentrations of ICG and then exposed to 780 nm light irradiation at a light fluence of 4 J/cm^2. Cell viability was measured by 3-(4,5-dimethylthiazol-2-yl)-2,5-diphenyltetrazolium bromide (MTT) assay 24 h after light exposure. Data are mean ± standard error of three replicates of each treatment.*

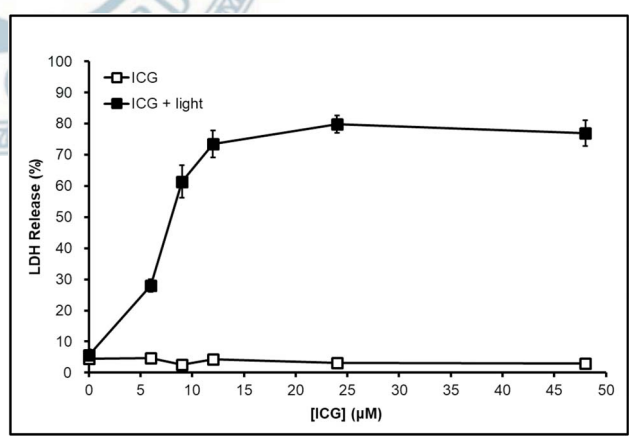

Figure 4. *Cytoxicity of rat smooth muscle (A-10) cells after photoactivation of indocyanine green (ICG). A-10 cells were incubated for 8 h in the presence of different concentrations of ICG and then exposed to 780 nm light irradiation at a light fluence of 4 J/cm^2. Cytotoxicity was measured by lactate dehydrogenase release assay 24 h after light exposure. Data are mean ± standard error of three replicates of each treatment.*

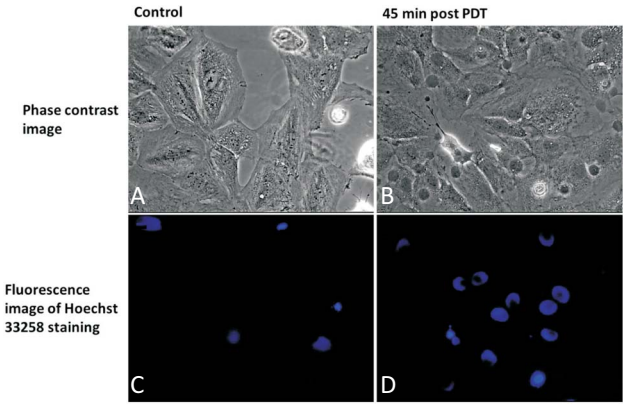

Figure 5. *Changes in nucleus morphology of rat smooth muscle (A-10) cells after photodynamic therapy (PDT) of indocyanine green (ICG). A-10 cells were incubated with 9 μM ICG for 8 h and then exposed to 780 nm light irradiation at a light fluence of 4 J/cm^2. The nucleus was stained with Hoechst 33258 (blue) 45 min after PDT and observed under a fluorescence microscope. (A) Representative image of control group (untreated) under bright-field. (B) Fluorescence image of control group. (C) Phase-contrast image of A-10 cells received PDT. Blebbing of cells was shown here. (D) Fluorescence image of A-10 cells received PDT. Perinuclear condensation was seen. Original magnification 400x.*

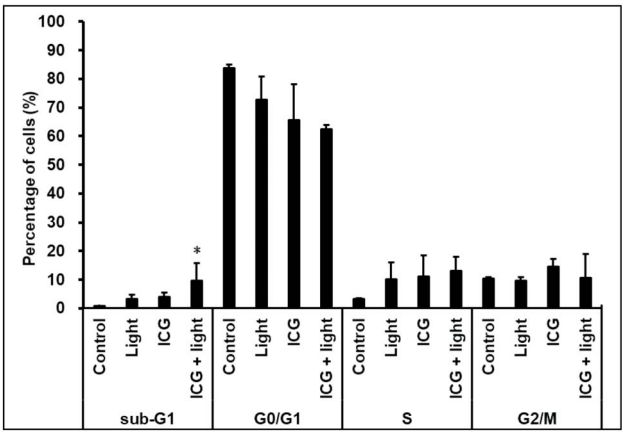

Figure 6. *Cell cycle analysis of rat smooth muscle (A-10) cells after photodynamic therapy (PDT) of indocyanine green (ICG). A-10 cells were incubated with 6 μM ICG for 8 h and then exposed to 780 nm light irradiation at a light fluence of 2 J/cm^2. Quantification of cell distribution in individual cell cycle phase was analyzed 12 h after PDT by flow cytometry. Bars represent mean ± standard error of three independent experiments. (*) signifies significant difference between medians of all groups (* $p < 0.05$).*

phases, respectively. The percentage (9.7%) of cells in the sub-G_1 phase in the ICG + light groups was significantly higher than that in the control group. Light or ICG treatment alone caused slight increases in cell apoptosis (sub-G_1 population) and reductions in G_0/G_1 population, however the medians of the control, ICG and light groups did not reach statistical significance in comparisons of the cell proportions at the sub-G_1 phase. A possible reason for this finding may be due to the slight enhancement in cytotoxicity after light or ICG treatment alone. The data indicated that ICG-PDT at a sub-lethal level might induce DNA-damage.

DISCUSSION

PDT using first- and second-generation photosensitizers to treat the intimal hyperplasia in rabbit or rat carotid arteries has been shown to provide beneficial effects.[37,38] We also previously demonstrated that PDT with ICG could inhibit intimal hyperplasia in a rat carotid artery injury model.[33] Since smooth muscle cells play a key role in the pathogenesis of restenosis after percutaneous coronary interventions, it is important to understand the direct effect of PDT with ICG on smooth muscle cells. Photosensitizers have been reported to be taken up in atherosclerotic plaques in some studies.[39-43] Investigations of ICG uptake by smooth muscle cells may shine a light on the inhibitory mechanism of ICG-PDT, and the intracellular accumulation of photosensitizers could be visualized using microscopy imaging.[26] In the present study, a dose-dependent increase in greenish ICG staining was observed in smooth muscle cells (Figure 1). This phenomenon has also been reported in studies of PDT with Zn(II)-phthalocyanine, protoporphyrin IX and chlorin e6 on vascular smooth muscle cells, which confirms the hypothesis that smooth muscle cells represent a major target during PDT treatment of carotid arteries to prevent restenosis.[26,44,45]

ICG absorbs strongly in the NIR spectrum, and thus it can convert absorbed NIR light energy into heat and ROS. It has been used in PDT for cancer treatment.[28,29,35,46] To determine the optimal timing of light irradiation for maximal PDT effect, the amount of intracellular ICG was evaluated by absorbance and fluorescence emission in the NIR spectrum. The maximum values of fluorescence intensity and absorbance intensity of ICG were found at 8 h of incubation with A-10 cells (Figure 2), which was an appropriate duration for photosensitizer incubation to obtain the data in this study.

The biocompatibility of ICG treatment on A-10 cells was tested using the MTT assay and LDH release assay.

The results showed that ICG did not have any dark toxicity on smooth muscles cells up to 48 μM (Figure 3 and 4). Upon exposure to 4 J/cm^2 NIR light, cell viability decreased and cell death increased in an ICG dose-dependent manner. The same tendency has been shown in many PDT studies with other photosensitizers in different cell lines.[26,35,44,47]

Changes in nuclear morphology and cell cycle distribution after PDT were further analyzed. At 45 min post-PDT, membrane blebbing and nuclear shrinkage were found (Figure 5). In addition, an increase in cells in the sub-G_1 phase was also observed (Figure 6). Our study indicate that apoptosis may be responsible for the inhibitory effect on A-10 cells by PDT using an ICG concentration less than IC_{50}. The mode of cell death caused by PDT could be affected by the concentration of ICG and the irradiant exposure, which has also been described in other cell types.[48,49] Our data (not shown) from annexin V and PI staining showed that most cells disappeared due to cell detachment or cell lysis after a high dose of ICG-PDT (20 μM ICG, 4 J/cm^2 NIR). Few cells remained on the cell culture surface that were stained with PI. Additional studies are necessary to elucidate the mode of cell death with ICG-PDT at different doses.

Apoptotic cell death can be triggered by intrinsic and extrinsic pathways. In general, PDT-mediated apoptotic pathways involve the activation of a cascade of caspases via mitochondrial pathways. ICG can also act as a photothermal agent which can convert optical energy to thermal energy.[35] PDT with a photothermal effect may induce cell death via a caspase-independent pathway mediated by endoplasmic reticulum.[48] Our data suggest that PDT may elicit apoptosis using an ICG concentration less than IC_{50}. Further studies are needed to clarify the pathways responsible for the apoptosis resulting from PDT.

CONCLUSIONS

In conclusion, the present study demonstrated that PDT using ICG and NIR light illumination was effective in suppressing viability and enhancing death of smooth muscle cells. The intracellular accumulation of ICG further supports the hypothesis that smooth muscle cells are a major target during PDT treatment of carotid arteries to prevent intimal hyperplasia. PDT may cause apoptosis using an ICG concentration less than IC_{50}. Further studies are needed to clarify the ICG-PDT related cell death pathways.

ACKNOWLEDGMENTS

This research was supported by grants from Taoyuan General Hospital, Ministry of Health and Welfare (grant number: PTH10413 and PTH10520) and Ministry of Science and Technology (grant number: MOST 106-2221-E-033-013), Taiwan, Republic of China.

CONFLICT OF INTEREST

All the authors declare no conflict of interest.

REFERENCES

1. Manabe I, Nagai R. Regulation of smooth muscle phenotype. *Curr Atheroscler Rep* 2003;5:214-22.
2. Mulvihill ER, Jaeger J, Sengupta R, et al. Atherosclerotic plaque smooth muscle cells have a distinct phenotype. *Arterioscler Thromb Vasc Biol* 2004;24:1283-9.
3. Mill C, George SJ. Wnt signalling in smooth muscle cells and its role in cardiovascular disorders. *Cardiovasc Res* 2012;95:233-40.
4. Geng YJ, Libby P. Progression of atheroma: a struggle between death and procreation. *Arterioscler Thromb Vasc Biol* 2002;22:1370-80.
5. Klouche M, Rose-John S, Schmiedt W, Bhakdi S. Enzymatically degraded, nonoxidized LDL induces human vascular smooth muscle cell activation, foam cell transformation, and proliferation. *Circulation* 2000;101:1799-805.
6. Rong JX, Shapiro M, Trogan E, Fisher EA. Transdifferentiation of mouse aortic smooth muscle cells to a macrophage-like state after cholesterol loading. *Proc Natl Acad Sci USA* 2003;100:13531-6.
7. Braun-Dullaeus RC, Mann MJ, Dzau VJ. Cell cycle progression: new therapeutic target for vascular proliferative disease. *Circulation* 1998;98:82-9.
8. Kim MS, Dean LS. In-stent restenosis. *Cardiovasc Ther* 2011;29:190-8.
9. Sung SH, Chen TC, Cheng HM, et al. Comparison of clinical outcomes in patients undergoing coronary intervention with drug-eluting stents or bare-metal stents: a nationwide population study. *Acta Cardiol Sin* 2017;33:10-9.
10. Yeh JS, Oh SJ, Hsueh CM. Frequency of vascular inflammation and impact on neointimal proliferation of drug eluting stents in por-

cine coronary arteries. *Acta Cardiol Sin* 2016;32:570-7.
11. Forrester JS, Fishbein M, Helfant R, Fagin J. A paradigm for restenosis based on cell biology: clues for the development of new preventive therapies. *J Am Coll Cardiol* 1991;17:758-69.
12. Welt FG, Rogers C. Inflammation and restenosis in the stent era. *Arterioscler Thromb Vasc Biol* 2002;22:1769-76.
13. Marx SO, Totary-Jain H, Marks AR. Vascular smooth muscle cell proliferation in restenosis. *Circ Cardiovasc Interv* 2011;4:104-11.
14. Chaabane C, Otsuka F, Virmani R, Bochaton-Piallat ML. Biological responses in stented arteries. *Cardiovasc Res* 2013;99:353-63.
15. Agostinis P, Berg K, Cengel KA, et al. Photodynamic therapy of cancer: an update. *CA Cancer J Clin* 2011;61:250-81.
16. Amemiya T, Nakajima H, Katoh T, et al. Photodynamic therapy of atherosclerosis using YAG-OPO laser and Porfimer sodium, and comparison with using argon-dye laser. *Jpn Circ J* 1999;63:288-95.
17. Kereiakes DJ, Szyniszewski AM, Wahr D, et al. Phase I drug and light dose-escalation trial of motexafin lutetium and far red light activation (phototherapy) in subjects with coronary artery disease undergoing percutaneous coronary intervention and stent deployment: procedural and long-term results. *Circulation* 2003; 108:1310-5.
18. Kou J, Dou D, Yang L. Porphyrin photosensitizers in photodynamic therapy and its applications. *Oncotarget* 2017;8:81591-603.
19. Yamaguchi A, Woodburn KW, Hayase M, et al. Photodynamic therapy with motexafin lutetium (Lu-Tex) reduces experimental graft coronary artery disease. *Transplantation* 2001;71:1526-32.
20. Waksman R, McEwan PE, Moore TI, et al. Photopoint photodynamic therapy promotes stabilization of atherosclerotic plaques and inhibits plaque progression. *J Am Coll Cardiol* 2008;52: 1024-32.
21. Usui M, Miyagi M, Fukasawa S, et al. A first trial in the clinical application of photodynamic therapy for the prevention of restenosis after coronary-stent placement. *Lasers Surg Med* 2004; 34:235-41.
22. Usui M, Asahara T, Naitoh Y, et al. Photodynamic therapy for the prevention of intimal hyperplasia in balloon-injured rabbit arteries. *Jpn Circ J* 1999;63:387-93.
23. Overhaus M, Heckenkamp J, Kossodo S, et al. Photodynamic therapy generates a matrix barrier to invasive vascular cell migration. *Circ Res* 2000;86:334-40.
24. Heckenkamp J, Aleksic M, Gawenda M, et al. Modulation of human adventitial fibroblast function by photodynamic therapy of collagen matrix. *Eur J Vasc Endovasc Surg* 2004;28:651-9.
25. Waterman PR, Overhaus M, Heckenkamp J, et al. Mechanisms of reduced human vascular cell migration after photodynamic therapy. *Photochem Photobiol* 2002;75:46-50.
26. Li Q, Cheng J, Peng C, et al. Apoptosis of vascular smooth muscle cells induced by photodynamic therapy with protoporphyrin IX. *Biochem Biophys Res Commun* 2010;391:69-72.
27. Yuan B, Chen N, Zhu Q. Emission and absorption properties of indocyanine green in intralipid solution. *J Biomed Opt* 2004;9: 497-503.
28. Chen WR, Adams RL, Higgins AK, et al. Photothermal effects on murine mammary tumors using indocyanine green and an 808-nm diode laser: an in vivo efficacy study. *Cancer Lett* 1996;98: 169-73.
29. Chen WR, Liu H, Carubelli R, Nordquist RE. Synergistic effect of photothermal and photoimmunological reactions in treatment of metastatic tumors. *J Xray Sci Technol* 2002;10:225-35.
30. Seo HM, Min HG, Kim HJ, et al. Effects of repetitive photodynamic therapy using indocyanine green for acne vulgaris. *Int J Dermatol* 2016;55:1157-63.
31. Genina EA, Bashkatov AN, Simonenko GV, et al. Low-intensity indocyanine-green laser phototherapy of acne vulgaris: pilot study. *J Biomed Opt* 2004;9:828-34.
32. Omar GS, Wilson M, Nair SP. Lethal photosensitization of wound-associated microbes using indocyanine green and near-infrared light. *BMC Microbiol* 2008;8:111.
33. Lin JS, Wang CJ, Li WT. Photodynamic therapy of balloon-injured rat carotid arteries using indocyanine green. *Lasers Med Sci* 2018.
34. Sato T, Ito M, Ishida M, Karasawa Y. Phototoxicity of indocyanine green under continuous fluorescent lamp illumination and its prevention by blocking red light on cultured Muller cells. *Invest Ophthalmol Vis Sci* 2010;51:4337-45.
35. Shirata C, Kaneko J, Inagaki Y, et al. Near-infrared photothermal/photodynamic therapy with indocyanine green induces apoptosis of hepatocellular carcinoma cells through oxidative stress. *Sci Rep* 2017;7:13958.
36. Eidet JR, Pasovic L, Maria R, et al. Objective assessment of changes in nuclear morphology and cell distribution following induction of apoptosis. *Diagn Pathol* 2014;9:92.
37. Eton D, Colburn MD, Shim V, et al. Inhibition of intimal hyperplasia by photodynamic therapy using photofrin. *J Surg Res* 1992; 53:558-62.
38. Ortu P, LaMuraglia GM, Roberts WG, et al. Photodynamic therapy of arteries. A novel approach for treatment of experimental intimal hyperplasia. *Circulation* 1992;85:1189-96.
39. Hsiang YN, Crespo MT, Richter AM, et al. In vitro and in vivo uptake of benzoporphyrin derivative into human and miniswine atherosclerotic plaque. *Photochem Photobiol* 1993;57:670-4.
40. Hsiang YN, Fragoso M, Tsang V, Schreiber WE. Determining the optimal dose of Photofrin in miniswine atherosclerotic plaque. *Photochem Photobiol* 1993;57:518-25.
41. Neave V, Giannotta S, Hyman S, Schneider J. Hematoporphyrin uptake in atherosclerotic plaques: therapeutic potentials. *Neurosurgery* 1988;23:307-12.
42. Palac RT, Gray LL, Turner FE, et al. Detection of experimental atherosclerosis with indium-111 radiolabelled hematoporphyrin derivative. *Nucl Med Commun* 1989;10:841-50.
43. Spokojny AM, Serur JR, Skillman J, Spears JR. Uptake of hematoporphyrin derivative by atheromatous plaques: studies in human in vitro and rabbit in vivo. *J Am Coll Cardiol* 1986;8:1387-92.
44. Wawrzynska M, Kalas W, Bialy D, et al. In vitro photodynamic therapy with chlorin e6 leads to apoptosis of human vascular

smooth muscle cells. *Arch Immunol Ther Exp (Warsz)* 2010;58: 67-75.
45. Magaraggia M, Visona A, Furlan A, et al. Inactivation of vascular smooth muscle cells photosensitised by liposome-delivered Zn(II)-phthalocyanine. *J Photochem Photobiol B* 2006;82:53-58.
46. Hirohashi K, Anayama T, Wada H, et al. Photothermal ablation of human lung cancer by low-power near-infrared laser and topical injection of indocyanine green. *J Bronchology Interv Pulmonol* 2015;22:99-106.
47. Montazerabadi AR, Sazgarnia A, Bahreyni-Toosi MH, et al. The effects of combined treatment with ionizing radiation and indocyanine green-mediated photodynamic therapy on breast cancer cells. *J Photochem Photobiol B* 2012;109:42-9.
48. Radzi R, Osaki T, Tsuka T, et al. Photodynamic hyperthermal therapy with indocyanine green (ICG) induces apoptosis and cell cycle arrest in B16F10 murine melanoma cells. *J Vet Med Sci* 2012; 74:545-51.
49. Radzi R, Osaki T, Tsuka T, et al. Morphological study in B16F10 murine melanoma cells after photodynamic hyperthermal therapy with indocyanine green (ICG). *J Vet Med Sci* 2012;74:465-72.

SUPPLEMENTARY INFORMATION

The nuclear morphology analyses using ImageJ software and similar approach of Eidet *et al.*[36] The result is shown in the figure on the right. Relative to the control, cells received ICG-PDT had smaller average nuclear area (61 ± 27%), and nuclear circumference (79 ± 19%), while nuclear form factor was similar (101 ± 39%). All the data of control and PDT groups did not reach statistical significance analyzed by Mann-Whitney test. Cell distribution was not analyzed due to unevenly distributed cells in both groups. We will consider performing the objective assessment in the future study.

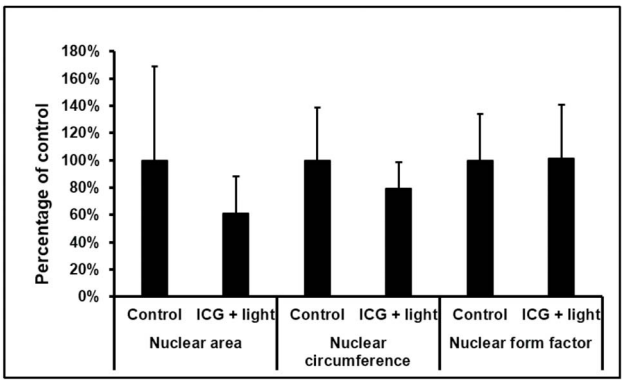

Supplementary figure. *Nuclear morphology analyses of rat smooth muscle (A-10) cells after ICG-PDT.*